Cancer Chemother Pharmacol (2011) 68:127–138
DOI 10.1007/s00280-010-1453-3

ORIGINAL ARTICLE

Novel small molecule drugs inhibit tumor cell metabolism and show potent anti-tumorigenic potential

Christina Trojel-Hansen · Kamille Dumong Erichsen · Mette Knak Christensen · Peter Buhl Jensen · Maxwell Sehested · Søren Jensby Nielsen

Received: 27 June 2010 / Accepted: 1 September 2010 / Published online: 18 September 2010

Abstract
Background Rapidly dividing tumor cells have an increased demand for nutrients to support their characteristic unabated growth; this demand is met by an increased availability of nutrients such as amino acids through vasculogenesis and by the enhanced cellular entry of nutrients through the upregulation of specific transporters. Deprivation of intracellular amino acids or block of amino acid uptake has been shown to be cytotoxic to many established human cancer cell lines in vitro and in human cancer xenograft models.
Results In this paper, we provide evidence that the two small molecule oxyphenisatine analogs TOP001 and TOP216 exert their anti-cancer effect by affecting tumor cell metabolism and inducing intracellular amino acid deprivation, leading to a block of cell proliferation. GCN2-mediated phosphorylation of eIF2α as well as mTOR pathway inhibition supports the above notion. In addition, these novel anti-cancer compounds inhibit DNA and protein synthesis and induce apoptosis in a broad spectrum of cancer cell lines. In vivo, the compounds induce tumor stasis and regression in mouse xenograft models of human breast, prostate, ovarian and pancreatic cancer, both when administered intravenously and orally.
Conclusion In conclusion, these small molecules, built on a 1,3-dihydroindole-2-one scaffold, elicit strong anti-proliferative and cytotoxic activity, and importantly, a strong anti-tumorigenicity is observed in in vivo xenograft models of human breast, ovary, prostate and pancreatic cancers encouraging the translation of this class of compounds into the clinic.

Keywords Small molecule · Anti-cancer · Xenograft · Cancer cells

Electronic supplementary material The online version of this article (doi:10.1007/s00280-010-1453-3) contains supplementary material, which is available to authorized users.

K. D. Erichsen · M. K. Christensen · P. B. Jensen
TopoTarget A/S, Symbion, Fruebjergvej 3,
2100 Copenhagen, Denmark

C. Trojel-Hansen (✉) · M. Sehested · S. J. Nielsen
XPU Bartholin, Rigshospitalet 3731, TopoTarget A/S,
Copenhagen Biocenter, Ole Maaløesvej 5,
2200 Copenhagen, Denmark
e-mail: chh@topotarget.com

Introduction

All mammalian cells regulate gene expression in response to changes in the external environment. Amino acid availability regulates cellular physiology by modulating gene expression and signal transduction pathways. The intracellular concentration of any given amino acid is governed by rates of amino acid influx and efflux via amino acid transporters, protein synthesis, protein turnover and aminoacyl-tRNA production, plus amino acid catabolism and biosynthesis. Mammalian cells have two recognized pathways for monitoring and responding to amino acid availability. These two pathways change the rate of protein synthesis in opposite directions [1–4]. The mammalian target of rapamycin (mTOR) pathway functions to confirm that a sufficient level of amino acids is present intracellularly in order to support protein synthesis and cell growth. The mTOR pathway is activated by numerous extracellular signals including growth factors and nutrients via the insulin/insulin-like growth factor (IGF1) 1/phosphatidyl inositol-3-OH kinase (PI(3)K) and extracellular signal–regulated kinase-p90 ribosomal protein S6 kinase (ERK-RSK) pathways [5–10]. However, amino acid depletion overrides all other mTOR

stimuli and results in pathway inhibition. Recent observations also indicate that Rag GTPases can physically interact with mTORC1 and regulate its sub-cellular redistribution in response to alterations in the levels of L-leucine [11–14]. Activation of mTOR ultimately results in the phosphorylation of p70 S6 kinase ($p70^{S6K}$) and 4E-BP1. Activation of $p70^{S6K}$ permits a high level of translation of mRNA species that encode ribosomal proteins, thereby maintaining protein synthesis and cell growth rates consistent with nutrient availability, whereas 4E-BP1 phosphorylation stimulates the translation of mRNAs with structured 5′ ends, such as those encoding for the growth regulators Myc and ODC [5]. In addition, amino acid deprivation regulates the protein synthesis at the level of an increase in the amount of un-charged tRNAs. This in turn leads to a binding of uncharged tRNAs to the general control non-derepressible protein 2 (GCN2) kinase resulting in its activation. Once activated, GCN2 kinase phosphorylates the translation initiation factor eIF-2a, which leads to a strong decrease in global protein synthesis [4, 15–17].

We here demonstrate that two compounds TOP001 and the optimized analog TOP216, belonging to a novel compound group based on a 1,3-dihydroindole-2-one scaffold, strongly inhibit the proliferation of cancer cell lines with striking selectivity (>1,000 fold) against cancer cell lines that are insensitive to the compounds [18]. In vivo, TOP001 and TOP216 show potent anti-cancer activity by inducing tumor regression (including cures) in mouse xenograft models of human tumors. We provide evidence that TOP216 may exert its function through depletion of intracellular amino acids. Treatment with TOP216 leads to the increased levels of phosphorylated eIF2α as well as decreased phosphorylation levels of mTOR substrates in sensitive cell lines, indicative of amino acid depletion. Taken together, these data suggest that TOP216 is able to deplete cancer cell lines of intracellular amino acids, despite the presence at high concentrations outside the cell. The control of amino acid provision is emerging as a powerful physiologic and pharmacologic mechanism for limiting cell proliferation. A deeper understanding of the mechanism of action of this interesting class of anti-cancer compounds may facilitate the progression into clinical trials and will lead to the validation of novel targets for anti-cancer therapy.

Materials and methods

Reagents and compounds

TOP001, TOP216 and TOP385 were synthesized as previously described [18]. TAXOL® was purchased from Bristol-Myers Squibb, 96-well black Packard Viewplates from (Perkin Elmer), Leucine uptake [^{14}C]Cytostar-T assay kit and [3H]Thymidine 5 mCi/mmol from (Amersham). Z-Val-Ala-D,L-Asp-flouromethylketone (zVADfmk) from (Bachem, Bubbendorf, Switzerland). Antibodies: phospho ACC(ser79), PathScan™ Multiplex Western Cocktail I: Phospho-p90RSK, Phospho-Akt, Phospho-p44/42 MAPK and Phospho-S6 Ribosomal, S6 ribosomal protein, S6 total protein; phospho p70 S6K (Thr389), phospho-eIF2α, eIF2α, phospho-GCN2 (Thr898), GCN2 (Cell Signaling Technology), GAPDH (Santa cruz).

Cell culture

All cell lines were obtained from ATCC (ATCC/LGC Promochem, Borås, Sweden). Cell culture reagents were obtained from Invitrogen except otherwise stated. All cell lines except MCF-10A were maintained according to American Type Culture Collection guidelines in RPMI medium containing 10% fetal bovine serum (FBS), 100 U/ml penicillin and 100 μg/ml streptomycin. MCF-10A was maintained in mammary epithelial growth medium (MEGM) with singlequot addition (BPE, hydrocortisone, hEGF, insulin, gentamicin/amphotericin-B) (Clonetics/Cambrex Bio Science, Walkersville, USA). For experiments, cells were trypsinized and seeded in 75-cm^2 flasks (Nunc) and allowed to grow overnight to reach 70% confluence at 37°C with 95%/5% air/CO_2 and 80% relative humidity. Cells were treated with drugs for indicated concentrations and periods. Cells were rinsed with PBS, harvested by scraping into PBS and isolated by centrifugation at 700×g for 5 min, and cell pellets were stored at −80°C until processing.

Western blot analysis

Cells were lysed in ELB containing 50 mM Hepes (pH 7), 250 mM NaCl, 5 mM EDTA, 0.1% Nonidet P-40, 10% glycerol, 0.5 mM DTT, 0.5 mM 4-(2-aminoethyl)benzenesulfonyl fluoride·HCl, 2 μg/ml leupeptin, 2 μg/ml aprotinin, 10 mM NaF and 50 mM β-glycerophosphate on ice for 15 min, sonicated for 5–10 s and centrifuged at 20,000×g for 15 min at 4°C. Protein extracts (20 μg, as determined by Bio-Rad Protein Assay (Bio-Rad)) were diluted in sample buffer (4 × Novex Nupage sample buffer), heated at 95°C for 5 min and separated by SDS–PAGE (4–12% and 3–8%)followed by blotting onto a nitrocellulose membrane using the NuPAGE-Novex Bis-Tris (XCell SureLockTM) system (Invitrogen). Membranes were blocked with 5% non-fat milk in Tris-buffered saline/0.1% Tween (TBS-T) for 1 h, incubated with primary antibody overnight at 4°C, washed three times 10 min in TBS-T and incubated with horseradish peroxidase–labeled secondary antibodies for 1 h at room temperature. The

membranes were then washed three times 10 min in TBS-T. Detection was achieved using ECL SuperSignal West Femto Maximum Sensitivity Substrate (Pierce) together with a ChemiDoc XRS/Quantity One documentation system (Bio-Rad).

Protein and DNA synthesis

Cells were seeded at 8.000 cells/well in 96-well Cytostar-T plates and cultured overnight at 37°C, 5% CO_2 in a humidified incubator. Growth medium was changed on the plates to 100 µl/well RPMI containing 10% FBS, 100 U/ml penicillin, 100 µg/ml streptomycin and 25 µg/ml gentamicin and [^{3}H]thymidine(0.4 µCi/well) or [^{14}C] leucine(0.5 µCi/ml), respectively. Compounds were diluted in growth medium containing 10% FCS. Compound dilutions were thereafter transferred to the cell plates by transfer of 100 µl/well resulting in a total volume of 200 µl/well containing final compound concentrations in 0.025% DMSO. Cell plates were incubated at 37°C, 5% CO_2 in a humidified incubator. Scintillation readings were made at 1 and 2 h the same cell plate by MicroBeta reader to determine the amount of [^{3}H]thymidine or [^{14}C]Leucine incorporated into DNA or protein, respectively.

Caspase assay

Cells were seeded at 8.000cells/well in 96-well black Packard Viewplates and cultured overnight at 37°C, 5% CO_2 in a humidified incubator. Growth medium was changed on the plates to 100 µl/well RPMI containing 10% FBS, 100 U/ml penicillin, 100 µg/ml streptomycin and 25 µg/ml gentamicin. Compounds were diluted in compound plates in growth medium containing 10% FCS. Compounds were thereafter transferred to the cell plates by transfer of 100 µl/well resulting in a total volume of 200 µl/well containing final compound concentrations in 0.025% DMSO. Cell plates were incubated with compounds at 37°C, 5% CO_2 in a humidified incubator. Caspase assays were run at 4, 6 or 22 h time-points, one plate per time-point. Caspase activity was measured using "Apo-ONE® Homogeneous Caspase-3/7 Assay" kit from Promega according to manufacture's instructions. Flourescence was read in a fluorescence plate reader using a 521-nm emission filter and a 499-nm excitation filter.

Viability and cell death assays

For AlamarBlue, cells were plated in black Packard/Perkin Elmer 96-viewplates. Cell densities were estimated based on growth during the assay to 80–90% confluency. The day after plating, the growth medium was changed on the plates to 100 µl/well RPMI containing 10% FBS, 100 U/ml penicillin, 100 µg/ml streptomycin and 25 µg/ml gentamicin. Compounds were diluted in growth medium containing 10% FCS. Compounds were thereafter transferred to the cell plates by transfer of 100 µl/well resulting in a total volume of 200 µl/well containing final compound concentrations in 0.025% DMSO. Terfenedine 50 µM was used as a control for maximal cell kill. Cell plates were incubated with compounds for 72 h at 37°C, 5%CO_2 and 95% humidity. The number of viable cells was estimated using AlamarBlue. AlamarBlue signal was read in a fluorescence plate reader using a 590-nm emission filter and a 530-nm excitation filter.

Cell viability and dose–response curves were measured by WST-1 proliferation assay (Roche) according to manufacturer's instructions and the setup described above. Apoptotic cells were determined in an Olympus IX microscope with the UV channel by counting condensed nuclei in cells stained with cell-permeable Hoeschst 33342 2,5 µg/ml (Sigma-Aldrich) for 10 min. Three randomly chosen fields containing a minimum of 100 cells were counted.

Clonogenic assay

In vitro colony forming assays were performed essentially to the same protocol as outlined in [19]. Briefly, cells were cultured with compounds and seeded onto 35-mm dishes in 3% (w/v) agar containing a sheep erythrocyte feeder layer. Agar plates were cultured for 14–21 days at 37°C and colonies counted using a digital colony counter and Sorcerer image analysis software (Perceptive Instruments Ltd, SuVolk, UK). Data were analyzed using GraphPad Prism (GraphPad Software, CA, USA) and Calcusyn (Biosoft, Cambridge, UK) as appropriate.

Metabolism study

Metabolon Inc. performed metabolic profiling and data analysis on thirty MCF-7 pellet samples consisting of six replicates of cells treated with 100 nM TOP216 or DMSO control. Cell pellets were analyzed at three time-points (0, 4.5 and 24 h), with $t = 0$ h being the time of drug administration. The extracted supernatant was split into equal parts for analysis on the GC and LC platforms. All samples were randomly distributed across a single-day platform run on GC/MS and LC/MS/MS instrumentation, and they were analyzed using Welch's two-sample *t*-test.

Xenograft studies

The anti-tumor effect of TOP216 in vivo was tested in a MCF-7, MDA-MB-468, A2780, MiaPaca and in a PC-3 subcutaneous (s.c.) xenograft models. 10e7 carcinoma cells in 200 µl RPMI medium were injected s.c. in Balb/c nude mice 24 h after whole body irradiation with a γ-source (2.0 Gy, Co^{60}).

The drinking water was complemented with 1.25 mg/ml of β-oestradiol (Sigma) to support the growth of hormone-dependent MCF-7 cells. Mice were randomized and treatment started at a mean volume of 194 ± 150 mm^3 (117 days after the graft). The study was performed by Oncodesign, France.

The PC-3 (CRL-1435, ATCC) human prostate cancer cells were grown in RPMI + 10% FBS and washed once with PBS, and 10e7 cells were suspended in 100 µl of PBS + 100 µl matrigel (BD) and injected s.c. in female NMRI/nude mice (Taconic). Treatment started at a mean volume of 403 ± 192 mm^3 (31 days after the graft). Oral treatment with TOP216 was given once weekly for 4 weeks. The study was performed by TopoTarget A/S, Denmark. TOP216 was formulated in 2% DMSO, 5% Tween80 and 93% isotonic saline and applied at 10 ml/kg (i.v. or p.o.). For i.v. treatment, the mice received 10 or 50 mg/kg/week, and for p.o. treatment, the mice received 100 mg/kg/week. In the MCF-7, MDA-MB-648, MiaPaca and A2780 study, paclitaxel (TAXOL®, 6 mg/ml, from Bristol-Myers Squibb), 15 mg/kg/week i.v. (5 ml/kg), was included as a positive control for tumor growth inhibition. Tumor diameters were measured during tumor growth and tumor volumes (Tv) estimated according to the formula: $Tv = (width^2 \times length)/2$.

Pharmacokinetics

A Water Quattro Premier LC–MS–MS system was used for bioanalysis. Plasma samples were precipitated with acetonitrile containing 1 µg/ml ^{13}C-labeled TOP216 (1:3), and separation from it major metabolite was performed by 0.05% formic acid–acetonitrile gradient on a Waters Sunfire C18 column (2.1 × 50 mm 3.5 um particles) operated at 40°C. Detection was performed by electrospray ionization in the positive mode (cone voltage 15.0 V and collision energy 15.0 V). A transition 354.10 > 260.10 m/z and 366.2 > 266.10 m/z was used for TOP216 and the internal standard, respectively. The linear range was from 70 ng/ml to 500 µg/ml ($r = 0.998$); the RSD for 5 repeated determinations in the range from 100 to 10,000 ng/ml was better, i.e., 12.1%, and accuracy ranged from 81 to 93%. Analysis of serum and hematologic parameters was performed by Oncodesign, France.

Results

Close analogs of the oxyphenisatin derivatives TOP216, TOP001 and TOP385 show similar anti-proliferative activities in the nM range

The anti-proliferative activity of the close analogs TOP001, TOP216 and TOP385 was tested on a broad spectrum of cancer cell lines using clonogenic assays, AlamarBlue and WST-1 proliferation assays (Table 1). TOP216, TOP001 and TOP385 showed the inhibition of cell proliferation at low nanomolar concentrations in drug-responsive cell lines as well as similar dose–response curves tested on MCF-7 and PC-3 cell lines (Fig. 1a and data not shown). The parental compound TOP001 was tested for dose–response inhibition of cell proliferation on a spectrum of human breast-derived non-cancerous and cancer cell lines: MDA-MB-231, MDA-MB-435S, MDA-MB-453, MDA-MB-468, SKBr-3, BT-474, BT-549, MCF-7, MCF-10A (non-cancerous), T-47D and ZR75-1. TOP001 induced a strong and dose-dependent inhibition of proliferation in this spectrum of cell lines, with MDA-MB-435 s, MDA-MB-231 and the non-cancerous cell line MCF-10A being highly insensitive (<1,000 fold when compared to sensitive lines) to the treatment TOP001 (Fig. 1b). The lead compound TOP216 was further analyzed in clonogenic assays for dose–response inhibition of cell proliferation of selected cell lines, MCF7, A2780, and the insensitive cell line MDA-MB-231(Data not shown) as well as the effect of TOP216 on cellular protein and DNA synthesis was measured (Fig. 1c). TOP216 treatment at 100 nM strongly inhibited protein synthesis and DNA synthesis rates in responsive MCF-7 cell line within 1–2 h as measured by leucine and thymidine incorporation, respectively. Effects of TOP001 and TOP216 on cell death markers and induction of cell death were also evaluated to establish whether the mechanism of inhibition of cell proliferation involves a cytostatic or cytotoxic mechanism (Fig. 1d, e). While a marked and rapid activation of caspase 3/7 was noted in cell lines such as BT-474, MCF-7, MDA-453, SK-BR-3 and T-47D, caspase activation was not apparent in non-responsive cell lines such as MDA-231 and MDA-435 and in the MDA-MB-468 cell line, although morphological alterations were noted. These data show that the TOP analogs exhibit pro-apoptotic effects in most drug-responsive human breast cancer cell lines and that the MDA-MB-468 cell line may represent an exception to this rule. The cytotoxic activity of TOP216 was investigated using Hoechst-33342 staining of apoptotic cells (Fig. 1e). Indeed, treatment with TOP216 at 200 nM for 20 h induced cell death of MCF-7 cells. Importantly, pre-treatment with the pharmacological general caspase inhibitor, z-VAD-fmk 100 µM, exhibited significant protection against TOP216-induced cell death (Fig. 1e). In conclusion, the TOP analogs dose dependently inhibit the cell proliferation at low nanomolar concentrations and induce caspase-dependent apoptosis of cancer cells.

The optimized analog TOP216 induces significant alterations in intracellular metabolite levels

To obtain further insight into the mechanism of action of the lead compound, we used metabolic profiling with the aim to

Table 1 Chemical structures and inhibition of tumor cell growth by TOP001, TOP216 and TOP385

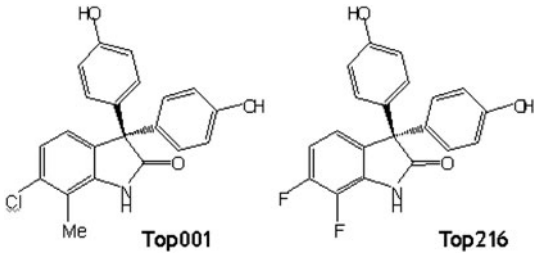

Species	Tissue	Status	Cell line	IC-50 (nM)	TOP001	TOP216	TOP385
Human	Prostate	Carcinoma	DU145		20	8	30
Human	Prostate	Carcinoma	LNCaP		30	8	
Human	Prostate	Carcinoma	PC3		22	8	22
Human	Glioma	Carcinoma	U-251		5,000	5,000	5,000
Human	Glioma	Carcinoma	LN18		5,000	5,000	5,000
Human	Glioma	Carcinoma	U87MG		30	9	200
Human	Melanoma	Carcinoma	LOX-IMVI		80	10	50
Human	Melanoma	Carcinoma	Malme 3 M		Inactive	Inactive	Inactive
Human	Colon	Carcinoma	HT29		1,000	500	500
Human	Colon	Carcinoma	HCT-15		90	15	40
Human	Colon	Carcinoma	SW620		Inactive	Inactive	Inactive
Human	Ovary	Carcinoma	OVCAR-3		7	3	10
Human	Ovary	Carcinoma	A2780		30	7	
Human	Ovary	Carcinoma	SK-OV-3		>1,000	>1,000	>1,000
Human	Lung	Carcinoma	NCI-H23		20	20	20
Human	Lung	Carcinoma	A549		Inactive	Inactive	Inactive
Human	Lung	Carcinoma	NCI-H226		1,000	50	300
Human	Mamma	Carcinoma	MDA-MB-231		Inactive	Inactive	Inactive
Human	Mamma	Carcinoma	MDA-MB-361		3	1	6
Human	Mamma	Carcinoma	T47D		7	3	11
Human	Mamma	Carcinoma	BT549		11	2	11
Human	Mamma	Carcinoma	MCF-7		10	4	20

The IC-50 values are in nanomolar scale

Cells were cultured with compounds and seeded onto 35-mm dishes in 3% (w/v) agar containing a sheep erythrocyte feeder layer. Agar plates were cultured for 14–21 days at 37°C and colonies counted using a digital colony counter and Sorcerer image analysis software (Perceptive Instruments Ltd, SuVolk, UK). Data were analyzed using GraphPad Prism The average IC_{50} values in nM scale represent mean values of at least three independent experiments carried out in triplicates

get an unbiased, global assessment of the action and effects of TOP216 by screening for changes in biochemical metabolites. This profiling was performed on sensitive MCF-7 cells treated with drug (100 nM) for 0, 4½ and 24 h, respectively. Full data curation of the MCF-7 pellets yielded 170 named metabolites. Welch's two-sample t-test was performed on the control group vs. drug-treated group and revealed that at 4.5 and 24 h, 71 and 112 metabolites, respectively, were significantly changed (P-value < 0.05), indicating that TOP216 treatment results in profound changes in intracellular metabolism and the choice of cellular energy source (Fig. 2).

Most notably TOP216 caused a dramatic reduction in intracellular amino acid levels, several as high as tenfold. Decreases in amino acids were more dramatic at 4.5 h compared to 24 h, as opposed to changes in sugars and lipids, which were more pronounced at 24 h.

Glucose and TCA cycle metabolites, such as citrate, alpha-ketoglutarate, succinate and malate, were all significantly increased in the TOP216 group (up to threefold), indicating that the drug altered the central energy metabolism of the cell.

Also, the nucleotide metabolites such as adenine, guanine, ATP, CMP and TMP were significantly increased in the TOP216 group at 24 h, whereas other nucleotide metabolites were significantly decreased, including hypoxanthine, inosine, adenosine, guanosine, uridine, AMP and UMP. These differences may be reflective of alterations in DNA/RNA synthesis or breakdown induced by TOP216.

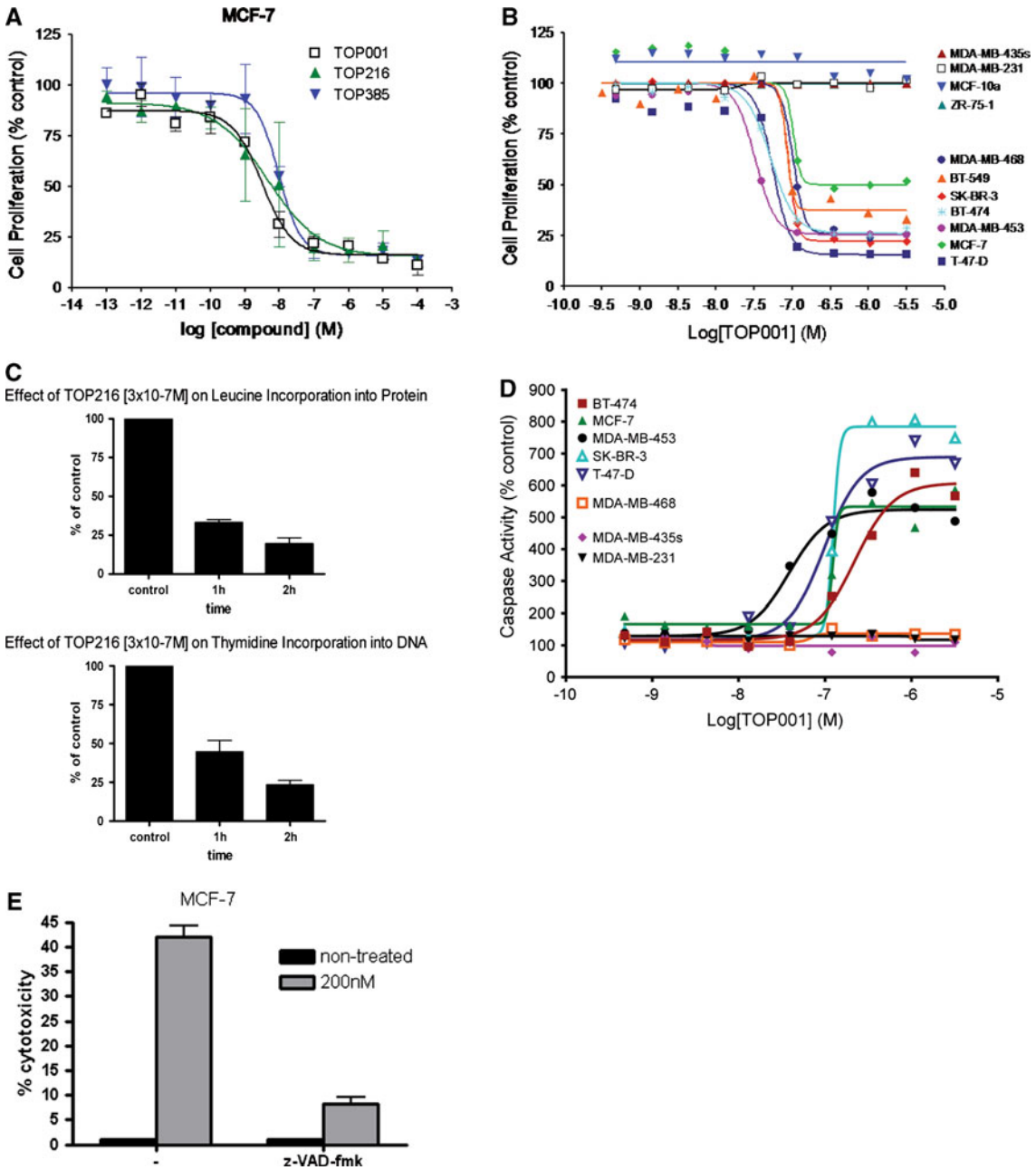

Fig. 1 TOP001 and TOP216 induce time- and dose-dependent inhibition of cell proliferation and cell death in a spectrum of human cancer cell *lines* **a** MCF-7 breast cancer cells were seeded at 3,000cellsl/well(96-well) 24 h before treatment with indicated concentrations of TOP001, TOP216 and TOP383 for 72 h. The viability of the cells was determined by WST-1 proliferation assay. **b** Dose–response curves for a panel of breast cancer cell *lines*. Cells were seeded at 3,000cells/well(96-well) 24 h before treatment with indicated concentrations of TOP001 for 72 h. The viability of the cells was determined by WST-1 proliferation assay. **c** Inhibition of protein and DNA synthesis by TOP216. MCF7 cells was seeded at 8.000cells/well(96-well) 24 h before addition of [3H]-thymidine or [14C]-Leucine and 100 nM TOP216. Scintillation readings were started after 1 h. Inhibition of protein and DNA synthesis is expressed as percentage of synthesis of non-treated cells. **d** Effects of TOP001 on caspase activation in human breast cancer cells. Caspase activity was measured using "Apo-ONE® Homogeneous Caspase-3/7 Assay" kit. **e** TOP216 induces caspase-dependent cell death of MCF-7 cancer cells. MCF-7 cells were left untreated or treated with 200 nM of TOP216 for 24 h before staining the DNA with membrane permeable Hoechst-33342. When indicated, the pan-caspase inhibitor zVAD-fmk (100 μmol/l) was added 1 h before TOP216. The viability of the cells was determined by counting apoptotic cells with condensed chromatin and is expressed as a percentage of untreated cells. TNF 10 ng/ml was used as positive control for cell death. Columns and graphs represent means of at least two independent experiments carried out in triplicate ($n = 6$)

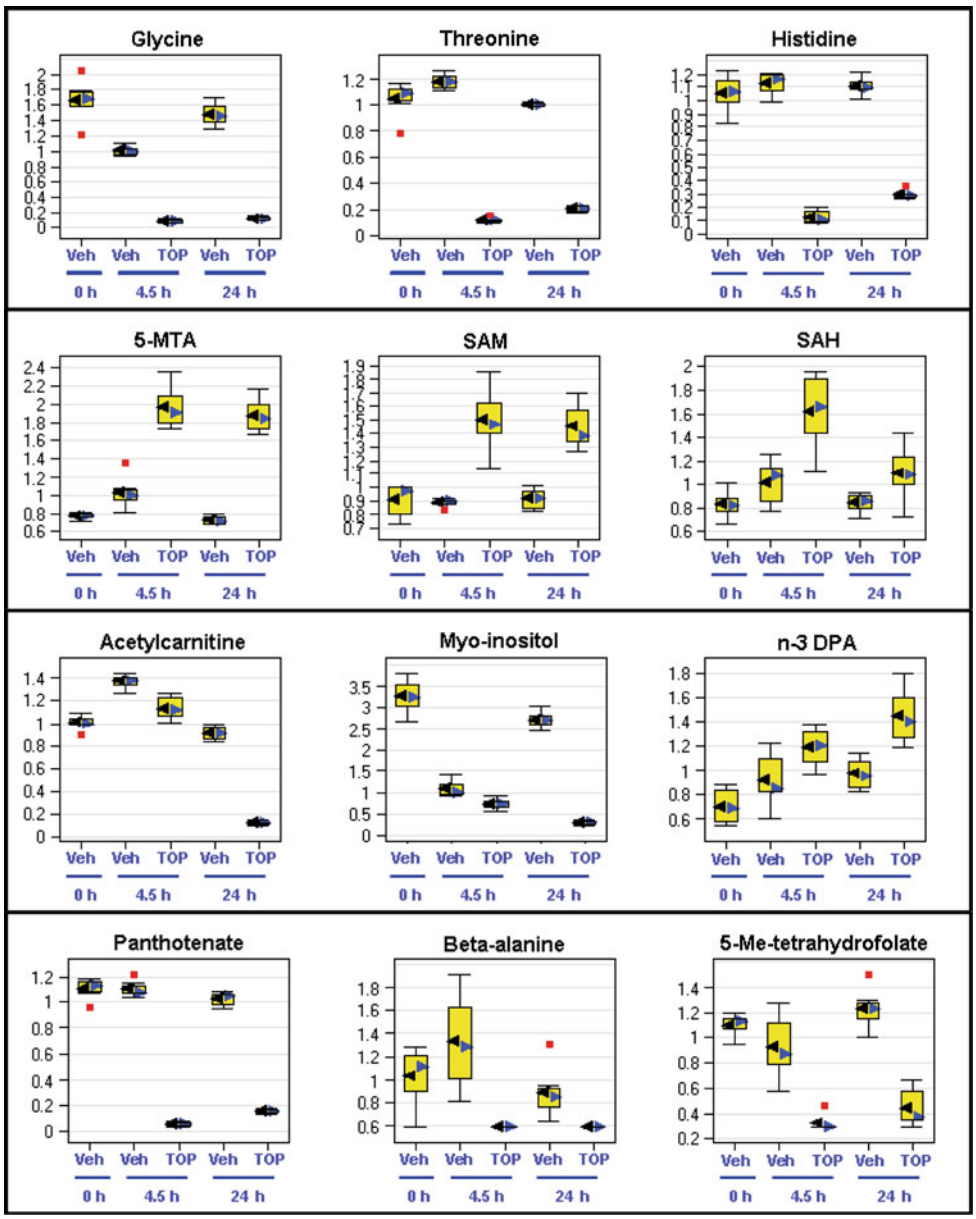

Fig. 2 TOP216 induces a significant decrease in intracellular amino acid levels and alters the levels of many metabolites. Fold changes after TOP216 treatment of MCF7 cells at 100 nM for 4.5 and 24 h are shown for selected significantly changed metabolites

5-methylthioadenosine (5-MTA) was significantly increased in the drug group, while the polyamines such as spermidine and putrescine were decreased. 5-MTA and polyamines are involved in the regulation of cell proliferation and apoptosis, which is in agreement with the drug affecting these pathways. Taken together, TOP216 dramatically affects the breast cancer cell metabolism, possibly as a result of the great reduction in intracellular amino acids rapidly induced by the drug.

TOP216 regulates mTOR and AMPK activity

The mTOR signaling pathway controls the rate of protein synthesis in response to intracellular amino acid levels by phosphorylation of its substrates p70S6K and 4EBP-1 [11, 14]. Based both on the dramatic effect of TOP216 on intracellular amino acid levels and energy metabolism, we hypothesized that this compound inhibits mTOR signaling. In agreement with this, TOP216 treatment (100 nM) of MCF7 cells caused a time-dependent decrease in the phosphorylation of p70S6K (Fig. 3a). As general energy metabolism was affected by the treatment with TOP216, we also investigated the activation status of AMP kinase, a key metabolic regulator and energy sensor, by phosphorylation status of its downstream effector, acetyl-CoA carboxylase (ACC). TOP216 treatment (100 nM) of MCF-7 cells over a 24-h time course caused a time-dependent increase in the phosphorylation levels of ACC (Fig. 3a).

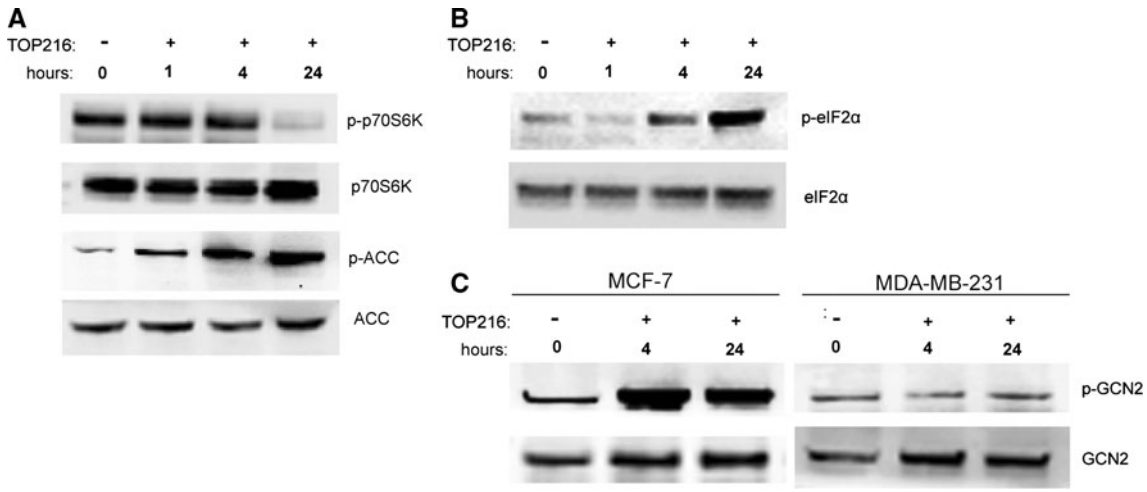

Fig. 3 TOP216 affects mTOR and GCN2 signalling. **a** Western blot analysis of phosphorylation status of p70S6K and ACC in protein samples from MCF7 cells. MCF7 cells were *left* untreated or treated for 1, 4 and 24 h, respectively, with 100 nM TOP216. **b–c** Effect of TOP216 (100 nM) GCN2 and eIF2α phosphorylation in MCF-7 and MDA-MB-231 cells over 24-h course. Levels p70S6K, ACC, GCN2 and eIF2α were used as internal control for individual experiments

Akt phosphorylation levels were not affected by the compound (data not shown) suggesting that AMPK activation and mTOR inhibition may be involved in the mechanism of inhibition of cancer cell growth by this compound, probably induced by the block of amino acid uptake.

TOP216 treatment activates the GNC2 amino acid sensing pathway

Under the conditions of amino acid deprivation, the translation initiation factor eIF2α is phosphorylated by GCN2. This strongly inhibits general protein synthesis while only allowing translation of few selected mRNAs [4, 16, 17]. Since mTOR inhibition generally leads to a mild decrease in overall protein synthesis and TOP216 strongly inhibited protein synthesis, the effect of TOP216 on regulating the activity of eIF2α was assessed by western blotting. Indeed, TOP216 treatment (100 nM) of MCF-7 cells over a 24-h time course showed a time-dependent increase in the phosphorylation levels of (Ser^{51}) eIF2α (Fig. 3b). Next we investigated whether the increased phosphorylation level of eIF2α was due to GCN2 activation as a result of uncharged tRNAs. In support with this notion, TOP216 treatment of MCF-7 cells leads to an induction of phosphorylated GCN2 (Fig. 3b). In addition, the levels of phosphorylated GCN2 in the insensitive cell line MDA-MB-231 were not increased in response to treatment with compound, indicating that activation of GCN2 is specific to the anti-proliferative mechanism of action of the compound (Fig. 3c). These results further support the observation that treatment with TOP216 affects the intracellular amino acid levels possibly by decreased amino acid uptake.

TOP216 shows strong anti-tumorigenic effect in vivo

The TOP216 compound was well tolerated in mice. In vivo safety studies of maximum tolerated doses in nude mice suggest no major adverse effects following oral, intraperitoneal (P.O.; I.P.) or intravenous (I.V.) administration using the highest feasible dose of the current formulations: 85 mg/kg (IV) and 17 0 mg/kg (oral). Lethality, body weight reduction or gross clinical signs were not observed following either single dose administration at 50, 66 and 100% of the highest feasible dose or multiple administration schedules (P.O. or I.P.; once daily for 14 days; I.V.; once weekly for 4 weeks). These data suggest that the maximum tolerated dose for P.O. administration of TOP216 is >170 and >85 mg/kg for I.V. administration. Clinical chemical analysis on serum samples revealed no abnormalities following dosing of animals with TOP216. Similarly, hematological analysis revealed no drug effects

Fig. 4 TOP216 induces pronounced tumor regression. 10e7 carcinoma cells in 200 µl RPMI medium were injected s.c. in Balb/c nude mice 24 h after whole body irradiation with a γ-source (2.0 Gy, Co60) **a** Pharmacokinetic profile of TOP216 in nude mice. **b** Effect of TOP216 at indicated doses (I.V. weekly for 4 weeks) on tumor volume in a MCF-7 breast cancer xenograft model in Balb/c mice, ($n = 8$). **c** Effect of TOP216 at indicated doses and taxol (5 mg/kg) in combination with TOP216 P.O. daily for 15 days on tumor volume in a MCF-7 breast cancer xenograft model in Balb/c mice, ($n = 8$) **d** Effect of TOP216, 100 mg/kg ×1 P.O./week ×4 weeks on large tumors in PC-3 prostate cancer xenograft model in Balb/c mice, ($n = 8$). **e** Effect of TOP216 at indicated doses, × 1 I.V./week × 4 weeks on tumor growth in PC-3 prostate cancer xenograft model in Balb/c mice, ($n = 8$). **f** Western blot analysis of phosphorylation status of p70S6K and eIF2α after treatment with TOP216 (I.V. 50 mg/kg) for 4, 24, 48 and 72 h of MCF-7 xenografts ▶

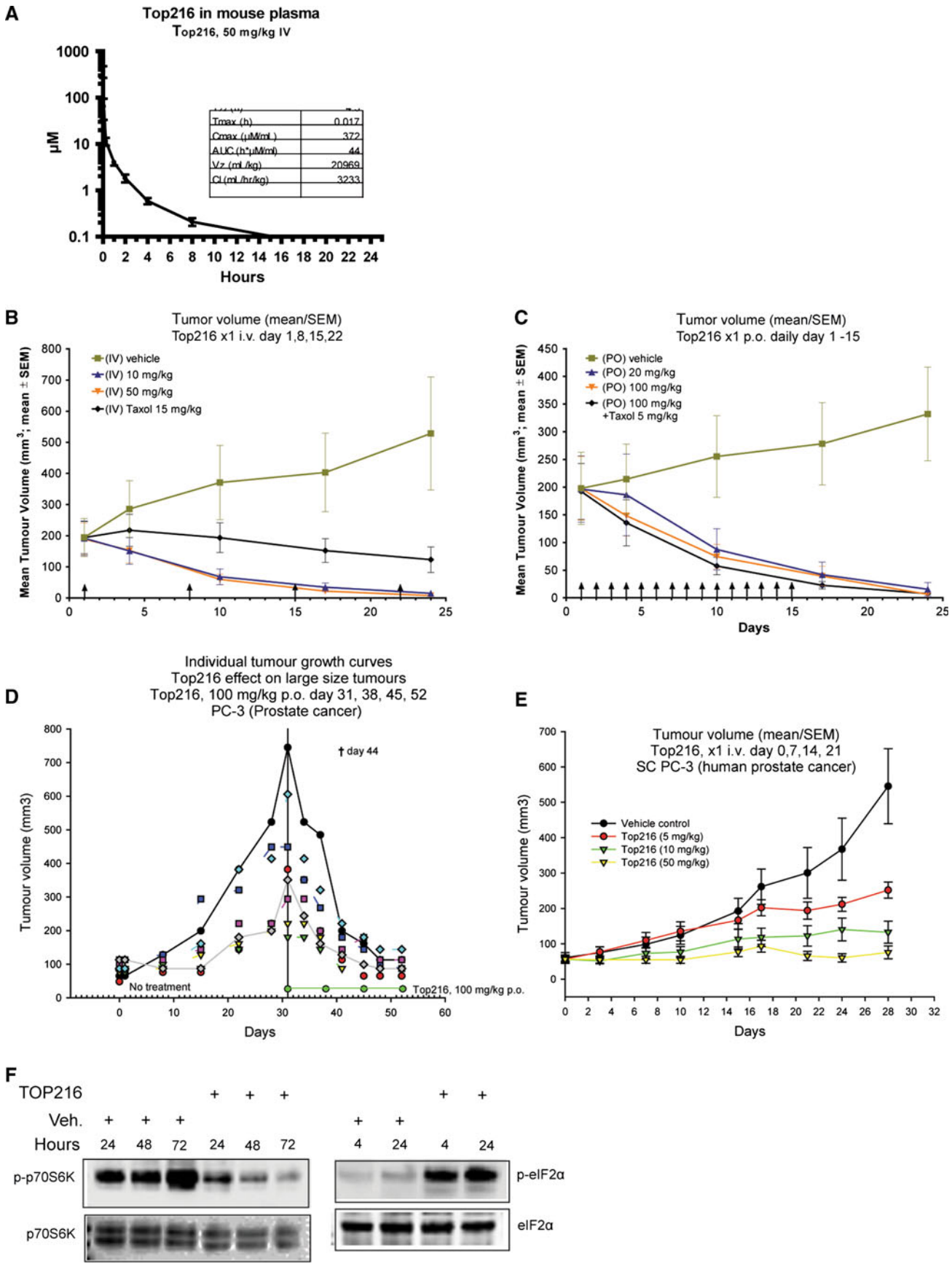
A
Top216 in mouse plasma
Top216, 50 mg/kg IV
Tmax (h) 0.017
Cmax (µM/mL) 372
AUC (h*µM/ml) 44
Vz (mL/kg) 20969
Cl (mL/hr/kg) 3233
µM
Hours
B
Tumor volume (mean/SEM)
Top216 x1 i.v. day 1,8,15,22
(IV) vehicle
(IV) 10 mg/kg
(IV) 50 mg/kg
(IV) Taxol 15 mg/kg
Mean Tumour Volume (mm3; mean ± SEM)
C
Tumor volume (mean/SEM)
Top216 x1 p.o. daily day 1 -15
(PO) vehicle
(PO) 20 mg/kg
(PO) 100 mg/kg
(PO) 100 mg/kg +Taxol 5 mg/kg
Mean Tumour Volume (mm3; mean ± SEM)
Days
D
Individual tumour growth curves
Top216 effect on large size tumours
Top216, 100 mg/kg p.o. day 31, 38, 45, 52
PC-3 (Prostate cancer)
† day 44
No treatment
Top216, 100 mg/kg p.o.
Tumour volume (mm3)
Days
E
Tumour volume (mean/SEM)
Top216, x1 i.v. day 0,7,14, 21
SC PC-3 (human prostate cancer)
Vehicle control
Top216 (5 mg/kg)
Top216 (10 mg/kg)
Top216 (50 mg/kg)
Tumour volume (mm3)
Days
F
TOP216
Veh.
Hours
24 48 72 24 48 72 4 24 4 24
p-p70S6K
p70S6K
p-eIF2α
eIF2α

on blood cell types, hemoglobin content or hematocrit using P.O. dosing. I.V. dosing also had no effect, although a reduction in platelet number was apparent in I.V. treatment groups, which appeared to be due to higher than expected platelet count in the vehicle control (Data not shown). LC-MS-MS was used for the bioanalysis of drug plasma content of TOP216 in nude mice. TOP216 was administered P.O. at increasing dose levels from 10 to 100 mg/kg. Plasma drug content was then analyzed in sequential blood samples collected 1 min–24 h following drug administration (Fig. 4a).

In nude mice carrying MCF-7 breast, PC-3 prostate (Fig. 4), MDA-MB-468 breast, A2780 ovary or MiaPaca pancreas (Supplementary Fig. 1) tumors, TOP216 was well tolerated and displayed significant anti-tumor activity. Both oral (P.O.; 20 and 100 mg/kg; Q1D×15; once daily for 15 days) and I.V. (10 and 50 mg/kg; Q1D×4; once weekly for 4 weeks) administration of TOP216 dramatically reduced MCF-7 tumor growth compared to vehicle control groups (Fig. 4b,c). The T/C value was 6–17% at the end of the P.O. treatment period; marked tumor regression was apparent in all animals ($n = 8$) with mean tumor volumes ~20% of the original size (For MDA-MB-468, A2780 and MiaPaca xenograft models see Supplementary Fig. 1). Tumor shrinkage continued after cessation of dosing (T/C values of 2–4%; tumor volumes <10% of original size). Using I.V. dosing, T/C values were 3 and 6% at the end of the administration period using 10 and 50 mg/kg TOP216, respectively (once weekly for 4 weeks). Marked tumor regression was noted at both doses in all animals; tumors were <10% of the original size. Paclitaxel treatment groups were included in the study for comparator purposes. Treatment with 15 mg/kg paclitaxel (IV; Q7D×4; weekly for 4 weeks) reduced tumor growth rate (T/C = 63% at termination of dosing) and resulted in less pronounced tumor regression. A combination group (100 mg/kg PO TOP216 + 5 mg/kg paclitaxel) was also included, but the extreme effects of TOP216 alone precluded meaningful analysis.

In the PC-3 model, TOP216 was given as an oral treatment (100 mg/kg/week) that was initiated at tumor sizes up to 750 mm^3. Tumor regression was observed after the first treatment, and regression continued during the treatment period with no tumor re-growth within the observation period of the experiment (until at least 35 days after the initial dose) (Fig. 4d). I.V (5–50 mg/kg) treatment in the PC3 xenograft model also resulted in tumor growth delay and regression (Fig. 4e).

MCF-7 xenografts treated with TOP216 for 4, 24, 48 and 72 h were furthermore subjected to analysis of eIF2α phosphorylation levels, and the activation status of the mTOR pathway was investigated using western blotting (Fig. 4f). Indeed, a rapid induction of the phosphorylation of eIF2α was observed in tumors taken out after 4- and 24-h treatment with TOP216 (50 mg/kg I.V.). In addition, the analyzed MCF-7 tumors showed the loss of mTOR pathway activation at 24, 48 and 72 h (Fig. 4f). Taken together, these data clearly show the potency and anti-tumorigenic potential of TOP216.

Discussion

TOP001 and the chemically optimized analogs TOP216 and TOP385 are structurally related members of a compound series with remarkable anti-cancer properties [18]. However, the mechanism of action by which this novel compound class mediates these strong anti-cancer and anti-proliferative effects is not clear.

The present study documents TOP001 and lead compound TOP216 as novel apoptosis inducing anti-cancer compounds that show the inhibition of cell proliferation at low nanomolar concentrations. Several studies have pointed to an important role of translational control in cancer development [20]. In addition to inhibiting cellular proliferation, we found that a functional consequence of TOP216 treatment of MCF-7 cells was a rapid and dramatic decrease in global protein and DNA synthesis.

The metabolome of a cancer cell is likely to show changes after responding to an anti-cancer drug [3, 21]. These changes can be used to explain observed effects of treatment of cell lines with the anti-cancer drug and eventually indicate its mechanism of action. A global assessment of the action and effects of TOP216 was therefore provided by screening for changes in biochemical metabolites. Strikingly, TOP216 induced a dramatic drop in intracellular amino acid levels, in several cases up to tenfold as measured after 4.5 h of TOP216 treatment of sensitive MCF-7 cells.

Deficiency of amino acids is sensed by the kinase GCN2 by a mechanism that involves uncharged tRNA binding to a regulatory HisRS domain, homologous to histidyl tRNA synthetase enzymes, within the kinase. This leads to auto-activation of its kinase domain and allows the phosphorylation of the translational initiation factor eIF2α, which in turn inhibits the recycling of eIF2α to its active GTP-bound form and thereby reduces general protein synthesis [4]. As expected from the observed metabolomic effects of the compound, treatment of the MCF-7 cell line with 100 nM TOP216 increased the phosphorylation of eIF2α and GCN2 supporting the above notion.

The mTOR signaling pathway also senses and responds to the amino acid levels, by controlling the rates of protein synthesis accordingly. Important substrates of mTOR are $p70^{S6K}$ and 4E-BP1. Both are consequently dephosphorylated during mTOR inhibition in response to low

intracellular amino acid levels, thereby leading to the inhibition of protein synthesis [14, 22]. TOP216 treatment of MCF-7 cells strongly decreased the phosphorylation levels of $p70^{S6K}$.

Interestingly, dysregulation of mTOR function via physiologic or mutational activation of upstream pathways is a common event in tumors from many linages. However, the clinical anti-tumor activity of mTORC1 inhibitor analogs such as rapamycin has been modest at best, since these drugs seem to primarily promote tumor growth stasis. O'Reilly et al. showed that mTORC1 inhibition leads to the activation of PI3 K/Akt and proposed this as a possible reason for the limited efficacy of rapamycin in epithelial cancers [23–25]. In contrast to mTORC1 inhibitors, the TOP analogs do not lead to the activation of Akt and inhibit translation both via mTOR and eIF2α supporting the strong in vivo efficacy of these drugs. TOP216 induced tumor stasis and regression (including cures) in mouse xenograft models of human breast, prostate, ovarian and pancreatic cancer, both when administrated intravenously and per-orally (Fig. 4 and Supplemental Fig. 2). Large PC-3, MCF-7, MDA-MB-468, Miapaca and A2780 tumors were shown to regress following per-oral and intravenous dosing of TOP216, respectively, and regression continued during the treatment period with no re-growth for as long as the animals were observed.

In addition to affecting mTOR activity, these data highlight a further important facet of cell biology, namely that amino acid provision can be used physiologically or pharmacologically to control cell proliferation. Interestingly, Paul Nicklin et al. recently showed that cellular uptake of L-glutamine by SLC15A is the rate-limiting step for essential amino acid—and growth factor regulation of mTORC1—as the bidirectional transporter SLC7A5/SCL3A2 uses intracellular L-glutamine as an efflux substrate to regulate the uptake of L-leucine, which subsequently leads to the activation of mTORC1. Previous studies have shown that, in general, human tumor cells are significantly more sensitive to amino acid deprivation than normal cells. There is widespread upregulation in human tumors of certain amino acid transporters, presumably to meet the increased demands for essential amino acids to take part in protein synthesis and cellular metabolism [3, 23]. It may be this increased demand for amino acids in tumor cells that underlies the effects of TOP216 and analogs. In conclusion, the strong inhibitory effect of the TOP216 on cancer cell proliferation, as well as the potent anti-tumorigenic effect on human tumor xenografts, suggests that these novel anti-cancer drugs, presumably targeting amino acid uptake, may represent new and useful tool in the treatment of human cancers. Extensive comparative studies in sensitive and insensitive cell lines with the aim of establishing the details of the mechanism of action of the TOP analogs and addressing the role of this compound group in amino acid transport are currently being carried out.

Conflict of interest None.

References

1. Kilberg MS, Pan YX, Chen H, Leung-Pineda V (2005) Nutritional control of gene expression: how mammalian cells respond to amino acid limitation. Annu Rev Nutr 25:59–85
2. Kimball SR, Jefferson LS (2006) New functions for amino acids: effects on gene transcription and translation. Am J Clin Nutr 83:500S–507S
3. Kroemer G, Pouyssegur J (2008) Tumor cell metabolism: cancer's Achilles' heel. Cancer Cell 13:472–482
4. Zhang P, McGrath BC, Reinert J et al (2002) The GCN2 eIF2alpha kinase is required for adaptation to amino acid deprivation in mice. Mol Cell Biol 22:6681–6688
5. Avruch J, Long X, Ortiz-Vega S, Rapley J, Papageorgiou A, Dai N (2009) Amino acid regulation of TOR complex 1. Am J Physiol Endocrinol Metab 296:E592–E602
6. Fingar DC, Blenis J (2004) Target of rapamycin (TOR): an integrator of nutrient and growth factor signals and coordinator of cell growth and cell cycle progression. Oncogene 23:3151–3171
7. Goberdhan DC, Boyd CA (2009) mTOR: dissecting regulation and mechanism of action to understand human disease. Biochem Soc Trans 37:213–216
8. Goberdhan DC, Ogmundsdottir MH, Kazi S et al (2009) Amino acid sensing and mTOR regulation: inside or out? Biochem Soc Trans 37:248–252
9. Huang J, Dibble CC, Matsuzaki M, Manning BD (2008) The TSC1-TSC2 complex is required for proper activation of mTOR complex 2. Mol Cell Biol 28:4104–4115
10. Huang J, Manning BD (2008) The TSC1-TSC2 complex: a molecular switchboard controlling cell growth. Biochem J 412:179–190
11. Hara K, Yonezawa K, Weng QP, Kozlowski MT, Belham C, Avruch J (1998) Amino acid sufficiency and mTOR regulate p70 S6 kinase and eIF-4E BP1 through a common effector mechanism. J Biol Chem 273:14484–14494
12. Sancak Y, Peterson TR, Shaul YD et al (2008) The rag GTPases bind raptor and mediate amino acid signaling to mTORC1. Science 320:1496–1501
13. Sancak Y, Sabatini DM (2009) Rag proteins regulate amino-acid-induced mTORC1 signalling. Biochem Soc Trans 37:289–290
14. Wang X, Campbell LE, Miller CM, Proud CG (1998) Amino acid availability regulates p70 S6 kinase and multiple translation factors. Biochem J 334(Pt 1):261–267
15. Sood R, Porter AC, Olsen DA, Cavener DR, Wek RC (2000) A mammalian homologue of GCN2 protein kinase important for translational control by phosphorylation of eukaryotic initiation factor-2alpha. Genetics 154:787–801
16. Wek RC (1994) eIF-2 kinases: regulators of general and gene-specific translation initiation. Trends Biochem Sci 19:491–496
17. Wek SA, Zhu S, Wek RC (1995) The histidyl-tRNA synthetase-related sequence in the eIF-2 alpha protein kinase GCN2 interacts with tRNA and is required for activation in response to starvation for different amino acids. Mol Cell Biol 15:4497–4506
18. Uddin MK, Reignier SG, Coulter T et al (2007) Syntheses and antiproliferative evaluation of oxyphenisatin derivatives. Bioorg Med Chem Lett 17:2854–2857

19. Roed H, Christensen IB, Vindelov LL, Spang-Thomsen M, Hansen HH (1987) Inter-experiment variation and dependence on culture conditions in assaying the chemosensitivity of human small cell lung cancer cell lines. Eur J Cancer Clin Oncol 23:177–186
20. Hanahan D, Weinberg RA (2000) The hallmarks of cancer. Cell 100:57–70
21. Vander Heiden MG, Cantley LC, Thompson CB (2009) Understanding the Warburg effect: the metabolic requirements of cell proliferation. Science 324:1029–1033
22. Nicklin P, Bergman P, Zhang B et al (2009) Bidirectional transport of amino acids regulates mTOR and autophagy. Cell 136:521–534
23. Easton JB, Kurmasheva RT, Houghton PJ (2006) IRS-1: auditing the effectiveness of mTOR inhibitors. Cancer Cell 9:153–155
24. O'Reilly KE, Rojo F, She QB et al (2006) mTOR inhibition induces upstream receptor tyrosine kinase signaling and activates Akt. Cancer Res 66:1500–1508
25. Wan X, Harkavy B, Shen N, Grohar P, Helman LJ (2007) Rapamycin induces feedback activation of Akt signaling through an IGF-1R-dependent mechanism. Oncogene 26:1932–1940